

Generic Contrast Agents

Our portfolio is growing to serve you better. Now you have a *choice*.



[VIEW CATALOG](#)

AJNR

This information is current as of May 30, 2025.

Diffuse Large B-Cell Epstein-Barr Virus–Positive Primary CNS Lymphoma in Non-AIDS Patients: High Diagnostic Accuracy of DSC Perfusion Metrics

A. Pons-Escoda, A. García-Ruíz, P. Naval-Baudin, F. Grussu, M. Viveros, N. Vidal, J. Bruna, G. Plans, M. Cos, R. Perez-Lopez and C. Majós

AJNR Am J Neuroradiol 2022, 43 (11) 1567-1574

doi: <https://doi.org/10.3174/ajnr.A7668>

<http://www.ajnr.org/content/43/11/1567>

Diffuse Large B-Cell Epstein-Barr Virus–Positive Primary CNS Lymphoma in Non-AIDS Patients: High Diagnostic Accuracy of DSC Perfusion Metrics

 A. Pons-Escoda,  A. García-Ruiz,  P. Naval-Baudin,  F. Grussu,  M. Viveros,  N. Vidal,  J. Bruna,  G. Plans,  M. Cos,  R. Perez-Lopez, and  C. Majós



ABSTRACT

BACKGROUND AND PURPOSE: Immunodeficiency-associated CNS lymphoma may occur in different clinical scenarios beyond AIDS. This subtype of CNS lymphoma is diffuse large B-cell and Epstein-Barr virus–positive. Its accurate presurgical diagnosis is often unfeasible because it appears as ring-enhancing lesions mimicking glioblastoma or metastasis. In this article, we describe clinicoradiologic features and test the performance of DSC-PWI metrics for presurgical identification.

MATERIALS AND METHODS: Patients without AIDS with histologically confirmed diffuse large B-cell Epstein-Barr virus–positive primary CNS lymphoma (December 2010 to January 2022) and diagnostic MR imaging without onco-specific treatment were retrospectively studied. Clinical, demographic, and conventional imaging data were reviewed. Previously published DSC-PWI time-intensity curve analysis methodology, to presurgically identify primary CNS lymphoma, was used in this particular lymphoma subtype and compared with a prior cohort of 33 patients with Epstein-Barr virus–negative CNS lymphoma, 35 with glioblastoma, and 36 with metastasis data. Normalized curves were analyzed and compared on a point-by-point basis, and previously published classifiers were tested. The standard percentage of signal recovery and CBV values were also evaluated.

RESULTS: Seven patients with Epstein-Barr virus–positive primary CNS lymphoma were included in the study. DSC-PWI normalized time-intensity curve analysis performed the best for presurgical identification of Epstein-Barr virus–positive CNS lymphoma (area under the receiver operating characteristic curve of 0.984 for glioblastoma and 0.898 for metastasis), followed by the percentage of signal recovery (0.833 and 0.873) and CBV (0.855 and 0.687).

CONCLUSIONS: When a necrotic tumor is found in a potentially immunocompromised host, neuroradiologists should consider Epstein-Barr virus–positive CNS lymphoma. DSC-PWI could be very useful for presurgical characterization, with especially strong performance of normalized time-intensity curves.

ABBREVIATIONS: AUC = area under the receiving operating characteristic curve; CE = contrast-enhanced; DLBC = diffuse large B-cell; EBV = Epstein-Barr virus; GE = gradient-echo; nTIC = normalized time-intensity curve; PCNSL = primary CNS lymphoma; PSR = percentage of signal recovery; rCBV = relative CBV; TIC = time-intensity curve; WHO = World Health Organization

Presurgical suspicion of CNS lymphoma is crucial for patient management. When it is suspected, initial corticosteroids

should be avoided, and biopsy instead of surgical resection is recommended.^{1,2}

Conventional imaging features of CNS lymphoma are widely described,^{3–7} but they mainly refer to primary CNS lymphoma

Received April 27, 2022; accepted after revision September 2.

From the Departments of Radiology (A.P.-E., P.N.-B., M.V., M.C., C.M.), Pathology (N.V.), and Neurosurgery (G.P.), Hospital Universitari de Bellvitge, Barcelona, Spain; Neurooncology Unit (A.P.-E., N.V., J.B., G.P., C.M.), Institut d'Investigació Biomèdica de Bellvitge-IDIBELL, Barcelona, Spain; Radiomics Group (A.G.-R., F.G., R.P.-L.), Vall d'Hebron Institut d'Oncologia, Barcelona, Spain; and Department of Radiology (R.P.-L.), Hospital Universitari Vall d'Hebron, Barcelona, Spain.

A.P.-E. and A.G.-R. are co-first authors of the manuscript. A.P.-E., P.N.-B., and C.M. created the experimental design. A.P.-E. led the investigation. A.P.-E. did the data collection. A.G.-R., F.G., and R.P.-L. led the data processing and statistical analysis in direct collaboration with A.P.-E., P.N.-B., and C.M. A.P.-E., P.N.-B., and C.M. wrote the manuscript and chose the best images. J.B. made important contributions to the final manuscript. A.P.-E. did the bibliographic research. M.V., M.C., N.V., G.P., and J.B. played an important role in imaging, patient data, or pathology sample acquisitions. All the authors have participated in the realization, review, and correction of the manuscript and its images, and all the authors have read and approved its submission to this journal.

This work was partially supported by a grant from the Instituto de Salud Carlos III (PI20/00360) to Carles Majós and Albert Pons-Escoda. Francesco Grussu has received funding from the postdoctoral fellowships program Beatriu de Pinós (2020 BP 00117), funded by the Secretary of Universities and Research (Government of Catalonia). Raquel Perez-Lopez is supported by a Prostate Cancer Foundation Young Investigator Award, CRIS Foundation Talent Award (TALENT-05), Fero Foundation, and the Instituto de Salud Carlos III.

Please address correspondence to Albert Pons-Escoda, MD, Radiology Department, Institut de Diagnòstic per la Imatge (IDI), Hospital Universitari de Bellvitge, C/Feixa Llarga SN, L'Hospitalet de Llobregat, 08907 Barcelona, Spain; e-mail: albert.pons.idi@gencat.cat; @PonsEscoda



Indicates article with online supplemental data.

<http://dx.doi.org/10.3174/ajnr.A7668>

(PCNSL), which specifically is Epstein-Barr virus (EBV)-negative and occurs in immunocompetent patients.⁸ However, less frequent subtypes of CNS lymphoma do not follow this imaging pattern. This is the case of immunodeficiency-associated CNS lymphoma, which usually appears as ring-enhancing lesions with central necrosis complicating accurate presurgical diagnosis.⁹⁻¹⁴

The World Health Organization (WHO) Classification of Tumors of the CNS includes B-cell and EBV-positivity as essential criteria for immunodeficiency-associated CNS lymphoma. Diffuse large B-cell (DLBC) EBV positive^{8,15} lymphoma is considered a distinct immunobiologic entity and represents nearly 10% of all CNS lymphomas.¹⁶ In the scientific literature, DLBC EBV-positive CNS lymphoma is mainly described in the context of AIDS. However, while the AIDS incidence is decreasing, other causes of immunodeficiency are increasing. This is the case for iatrogenesis (treatment-induced immunosuppression) in the context of post-transplantation or for other causes such as autoimmune diseases, or even for other situations such as immunosenescence and chronic inflammation.¹⁷⁻²¹

DSC-PWI is a quantitative MR imaging technique that has shown promising results for presurgical identification of PCNSL. This tumor shows a characteristic time-intensity curve (TIC), which can be precisely evaluated with a new methodology that renders normalized TICs (nTICs)^{22,23} as well as by a lower relative CBV (rCBV) and a higher percentage of signal recovery (PSR) than glioblastoma or metastasis.^{22,24-30} However, to the best of our knowledge, there is very little literature regarding DSC-PWI features specific to DLBC EBV-positive CNS lymphoma.¹⁰

In summary, DLBC EBV-positive CNS lymphoma constitutes a unique clinical immunobiologic entity with particular imaging features that challenge its presurgical diagnosis. Conventional imaging is usually misleading, and comprehensive analysis of the full potential of DSC-PWI in this scenario is lacking.

In this article, the clinical and radiologic features of a homogeneous data set of patients with DLBC EBV-positive CNS lymphoma without AIDS are comprehensively described. The main objective of the study was to test the performance of DSC-PWI metrics (nTIC, PSR, CBV) for the presurgical differentiation of this entity from glioblastoma and metastasis.

MATERIALS AND METHODS

The research ethics committee of the Hospital Universitari de Bellvitge tertiary center approved this retrospective study and issued a waiver for a specific informed consent. Patient data were protected and anonymized in accordance with European Union General Data Protection Regulation legislation.

Patients

Records of patients with confirmed primary DLBC EBV-positive CNS lymphoma (December 2010 to January 2022) were retrieved from our center's database. Inclusion criteria were the following: 1) confirmed tumor diagnosis by histology (2016 WHO lymphoid neoplasm¹⁵ and 2021 WHO CNS tumor⁸ classification); 2) extension study without evidence of systemic lymphoma; and 3) available diagnostic MR imaging examination without onco-specific treatment.

Relevant clinical and demographic data were retrieved from the hospital records, including age, sex, underlying conditions, radiologic diagnosis, histopathologic diagnosis, and initial diagnostic-therapeutic patient management.

For comparison of the obtained perfusion metrics, we retrieved DSC-PWI data from previously published²² cases of EBV-negative PCNSL, glioblastoma, and metastasis, which are balanced by technique and demographic characteristics, as well as quality-filtered.

Imaging

The MR images included in the study were acquired in a single center with 1 of 2 scanners, either an Ingenia 1.5T or an Intera 1.5T (Philips Healthcare), both using a 16-channel head coil. MR imaging examinations included T1WI, contrast-enhanced (CE) T1WI, TSE-T2WI, gradient-echo (GE) T2*WI, DWI, and DSC-PWI.

Conventional Imaging. Two experienced neuroradiologists from our tertiary reference center neuro-oncology unit, A.P.-E. and C.M., with >8 and 25 years of experience in neuro-oncologic radiology, respectively, visually assessed T1WI, CE-T1WI, TSE-T2WI, GE-T2*WI, and DWI sequences. The assessment was done independently and included the number of lesions, location, ring enhancement, TSE-T2WI signal intensity, GE-T2*WI hemorrhagic components, and diffusion restriction. Discrepancies were resolved by consensus.

Perfusion Imaging Acquisition. Two GE DSC-PWI sequences were used. The first (2 cases) included 40 dynamic volumes with a temporal resolution of 1.9 seconds with the following parameters: flip angle = 7°, TE = 25–30 ms, TR = 16–20 ms, in-plane resolution = 1.72 mm, and section-thickness = 1.5 mm. The second (5 cases) included 60 dynamic volumes with a temporal resolution of 1.6 seconds with flip angle = 75°, TE = 40 ms, TR = 1522–1771 ms, pixel spacing = 1.75 mm, and section thickness = 5 mm. The intravenous contrast was gadobutrol, 1 mmol/mL, 0.1 mmol/kg. No contrast preload administered. Baseline acquisition was on the order of 10 points. The start of the automatic injection (4–5 mL/s) was by a manual setting.

Postprocessing. The segmentations of enhancing tumor and contralateral normal-appearing WM were performed on CE-T1WI semiautomatically (histogram intensity thresholding) and coregistered with DSC-PWI. Necrosis was not included in the segmentations. Segmentations were performed on 3D Slicer, Version 4.10 (<http://www.slicer.org>), and coregistration was with the BRAINSFit module (3D Slicer). TICs were preprocessed using the method proposed by Pons-Escoda et al,^{22,23} which renders nTICs: Signal-intensity values of the enhancing tumor TIC were normalized by dividing by the maximal signal intensity drop of the normal-appearing WM, and time values were normalized as relative to the period of the descending curve on normal-appearing WM. The resultant nTICs are time- and intensity-normalized, making them comparable among patients. The TICs were processed using Python 3.6 software (<https://www.python.org/downloads/release/python-360/>).

Visual evaluation of the average curves and point-by-point statistical comparison (Mann-Whitney *U* test) were performed.

Table 1: Clinical overview of the included patients with pathology-confirmed DLBC EBV-positive CNS lymphoma

| | Age (yr) | Sex | Underlying Conditions | Radiologic Diagnosis ^a | Diagnostic-Therapeutic Initial Management |
|-----|----------|--------|--|--|--|
| P 1 | 66 | Male | Kidney transplant | Multiple metastases ^b | Biopsy: reason, multiple lesions |
| P 2 | 76 | Male | Chronic myeloproliferative disorder; essential thrombocythemia | Glioblastoma | Biopsy: reason, patient basal clinical status |
| P 3 | 74 | Male | Liver transplant | Single metastasis ^c | Biopsy: reason, second-look radiologic opinion |
| P 4 | 62 | Female | Systemic sclerosis and discoid cutaneous lupus | Glioblastoma | Maximal safe surgical resection |
| P 5 | 70 | Female | Immunosenescence | Multiple metastases or multifocal glioblastoma | Biopsy: reason, multiple lesions |
| P 6 | 63 | Male | Autoimmune hepatitis | Metastasis or glioblastoma | Maximal safe surgical resection |
| P 7 | 78 | Female | Kidney transplant | Single metastasis | Maximal safe surgical resection |

Note:—P indicates patient.

^a Based on a radiologic report from our neuro-oncology reference tertiary university hospital.

^b Atypical infection was considered, but as an unlikely option.

^c A second-look opinion raised the possibility of atypical lymphoma.

Table 2: Radiologic overview of the included patients with pathology-confirmed large B-cell EBV-positive primary CNS lymphoma

| | No. | Location | Necrosis | CE-T1WI Ring | T2WI Solid Parts | T2*WI Hemorrhage | DWI Solid Parts |
|-----|----------|---|----------|-----------------------------|----------------------------|------------------|----------------------------|
| P 1 | Multiple | Bilateral basal ganglia and cortico-subcortical | Yes | Irregular thick and nodular | Heterogeneous hyperintense | Moderate | Heterogeneous restricted |
| P 2 | Single | Parietal corticosubcortical | Yes | Irregular thick | Heterogeneous intermediate | Subtle | Heterogeneous intermediate |
| P 3 | Single | Frontal cortico-subcortical | Yes | Irregular thick | Heterogeneous hypointense | Moderate | Heterogeneous restricted |
| P 4 | Single | Parietal cortico-subcortical | Yes | Irregular thick | Heterogeneous hyperintense | Prominent | Heterogeneous restricted |
| P 5 | Multiple | Cortico-subcortical unilateral | Yes | Irregular thin | Heterogeneous hypointense | Prominent | Heterogeneous intermediate |
| P 6 | Single | Basal ganglia | Yes | Irregular thick | Homogenous hypointense | Prominent | Heterogeneous restricted |
| P 7 | Single | Frontal subcortical | Yes | Regular thin | Homogenous hypointense | Moderate | Homogeneous restricted |

Two previously published classifiers to differentiate PCNSL from glioblastoma and metastasis through nTICs were used to assess the performance in the particular group of DLBC EBV-positive CNS lymphomas.²² Also, we assessed the performance of mean rCBV and PSR. rCBV was obtained after leakage correction and normalized to the contralateral normal-appearing WM³¹ with 3D Slicer, Version 4.10, and PSR was obtained as described by Cha et al.³²

Additionally, replicating the same prior methodology²² (logistic binary regression on the 5 most discriminatory points of the curve), we trained a 1-way nTIC model to differentiate PCNSL and glioblastoma/metastasis as a single group and tested it for DLBC EBV-positive CNS lymphoma.

RESULTS

Patients

Seven patients fulfilled the inclusion criteria and were included in the study (4 men; mean age, 70 years; range, 62–78 years). The underlying conditions were the following: 3 iatrogenic in the context of posttransplant, 2 iatrogenic in the context of autoimmune disease, 1 chronic inflammation, and 1, elderly, related to immunosenescence.^{15,17,19–21} The original radiologic diagnosis

was metastasis or glioblastoma in all patients. Initial biopsy was recommended in 4 cases, while the remaining patients were candidates for initial maximal safe resection. Patient characteristics are specified in Table 1. Four patients with DLBC EBV-positive CNS lymphoma were on corticosteroids at the time of MR imaging.

For perfusion metrics comparisons, DSC-PWI data from 33 patients with EBV-negative primary CNS lymphomas, 35 with glioblastomas, and 36 patients with metastases (total, 104; fifty-five men; mean age, 60 years; range, 18–82 years) were included. These data were previously acquired in the same center, with same technical parameters,²² and there were no significant differences in their distributions with the currently analyzed cohort (χ^2 test, $P = .108$).

Imaging

Conventional Imaging. Conventional imaging findings are shown in Table 2. The most relevant findings on MR imaging were the following: single lesions and peripheral cortico-subcortical location; necrotic lesions with ring enhancement and different degrees of hemorrhage; and heterogeneous signal on DWI (Table 2 and Fig 1). An unexpected TSE-T2 heterogeneously iso-/hypointense signal of the central nonenhancing content of lesions was also described.

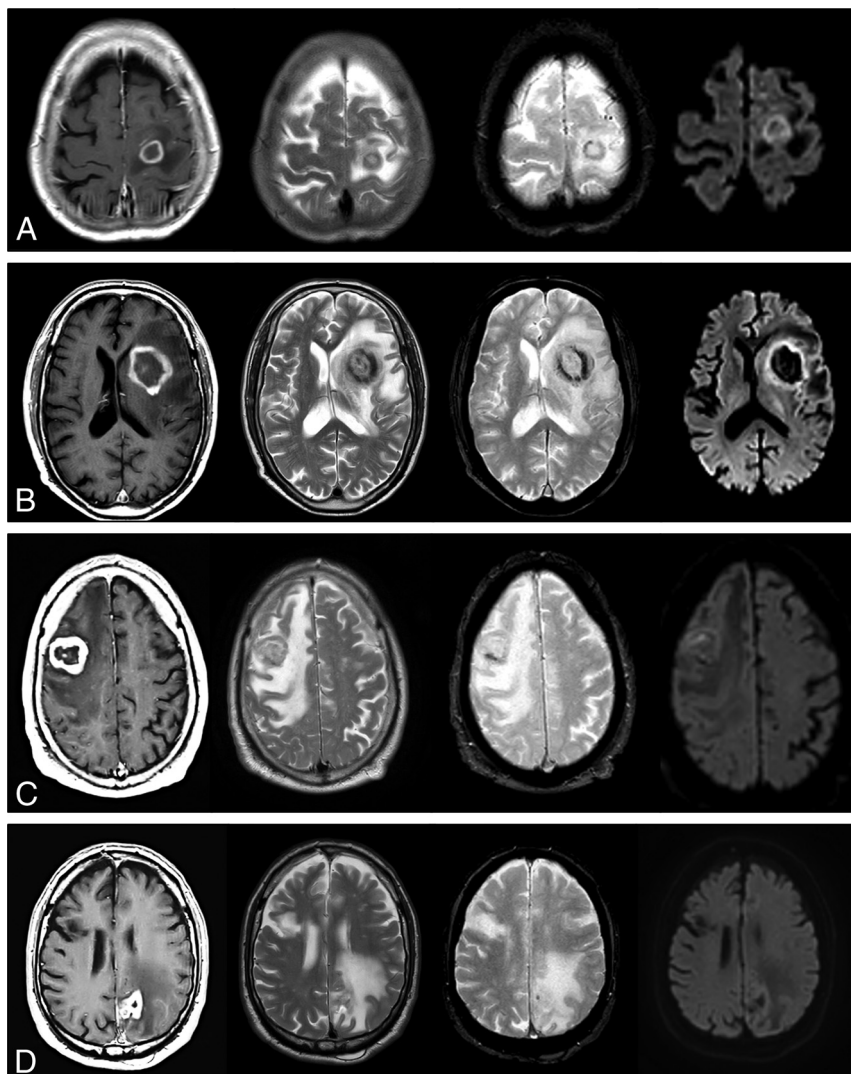


FIG 1. Visual summary of MR imaging features in 4 patients with pathology-confirmed DLBC EBV-positive CNS lymphoma. One patient in each row: CE-T1WI, TSE-T2WI, GE-T2*WI, and DWI at $b = 1000$. Regular thin ring enhancement of a subcortical lesion in A, irregular thick ring enhancement of a basal-ganglia lesion in B. The solid walls of lesions show homogeneous TSE-T2WI low signal and restricted diffusion. Incidental right frontal chronic infarct in D. Irregular thick ring enhancement in cortico-subcortical lesions: frontal in C, parietal in D. Heterogeneous signal on TSE-T2WI: hypointense in C, iso- to hyperintense in D. Intermediate heterogeneous signal on DWI. Different amounts of hemorrhage in all cases are depicted by the GE-T2*WI. Note the TSE-T2WI heterogeneous iso- to hypointense signal of the nonenhancing central content of tumors in A–C, especially in B and C.

Perfusion Imaging. Figure 2 overlays the average nTIC for DLBC EBV-positive CNS lymphoma, PCNSL (EBV-negative), metastasis, and glioblastoma. Few differences were detected between DLBC EBV-positive CNS lymphoma and PCNSL. The most relevant visual differences with metastasis or glioblastoma were seen around the maximal-signal-intensity drop and signal-recovery segments of the curves. The Mann-Whitney *U* test found significant differences between DLBC EBV-positive CNS lymphoma and glioblastoma or metastasis at almost all time points of the curve, with the greatest level around the maximal-signal-intensity drop and signal-recovery segments, reinforcing the visual assessment.

Results of the 2 previously published classifier algorithms,²² along with the classification potential of PSR and rCBV, can be

found in Table 3, Fig 3, and the Online Supplemental Data. The 2 nTIC algorithms showed the most significant differences ($P < .001$ for glioblastoma and metastasis) and the best classification results. For glioblastoma, they yielded an area under the receiver operating curve (AUC) of 0.984, accuracy of 0.93, sensitivity of 1.0, and specificity of 0.91, while for metastasis, they yielded an AUC of 0.898, accuracy of 0.82, sensitivity of 1.0, and specificity of 0.78. Additionally, PSR was also significant for both comparisons, albeit slightly less so ($P < .01$ for both, AUC = 0.833 and 0.873). Finally, rCBV yielded significant differences for DLBC EBV-positive CNS lymphoma against glioblastoma ($P = .003$, AUC = 0.855), but not against metastasis ($P = .122$, AUC = 0.687).

Furthermore, when we compared DLBC EBV-positive CNS lymphoma and PCNSL, visual assessment of average nTICs showed very similar morphology, and statistical comparison confirmed no significant differences between them in the Mann-Whitney *U* test. Moreover, no significant differences were found in PSR, while rCBV showed a barely significant difference ($P = .05$). All results are summarized in Table 3, Fig 3, and the Online Supplemental Data.

Last, the 1-way adapted classifier results can be found in the Online Supplemental Data. The nTIC algorithm (Online Supplemental Data) discriminated between DLBC EBV-positive CNS lymphoma and glioblastoma/metastasis as a whole, with AUC = 0.90, while the AUC was 0.85 for PSR and 0.77 for rCBV.

No significant differences were found in all time points of nTICs, CBV, or PSR values among the different DSC-PWI techniques (Mann-Whitney *U* test, P values = .245–1), neither among patients with nor without corticosteroids at the time of MR imaging (Mann-Whitney *U* test, P values = .157–.724).

DISCUSSION

In this study, we present a unique cohort of 7 patients with DLBC EBV-positive CNS lymphoma without AIDS in whom DSC-PWI was performed and compare them with those with PCNSL (EBV-negative), glioblastoma, and metastasis. While conventional imaging was misleading due to the strong similarity between DLBC EBV-positive CNS lymphoma and glioblastoma or metastasis, DSC-PWI metrics provided promising results, the best determined by nTIC analysis. Moreover, this is the first study to describe and

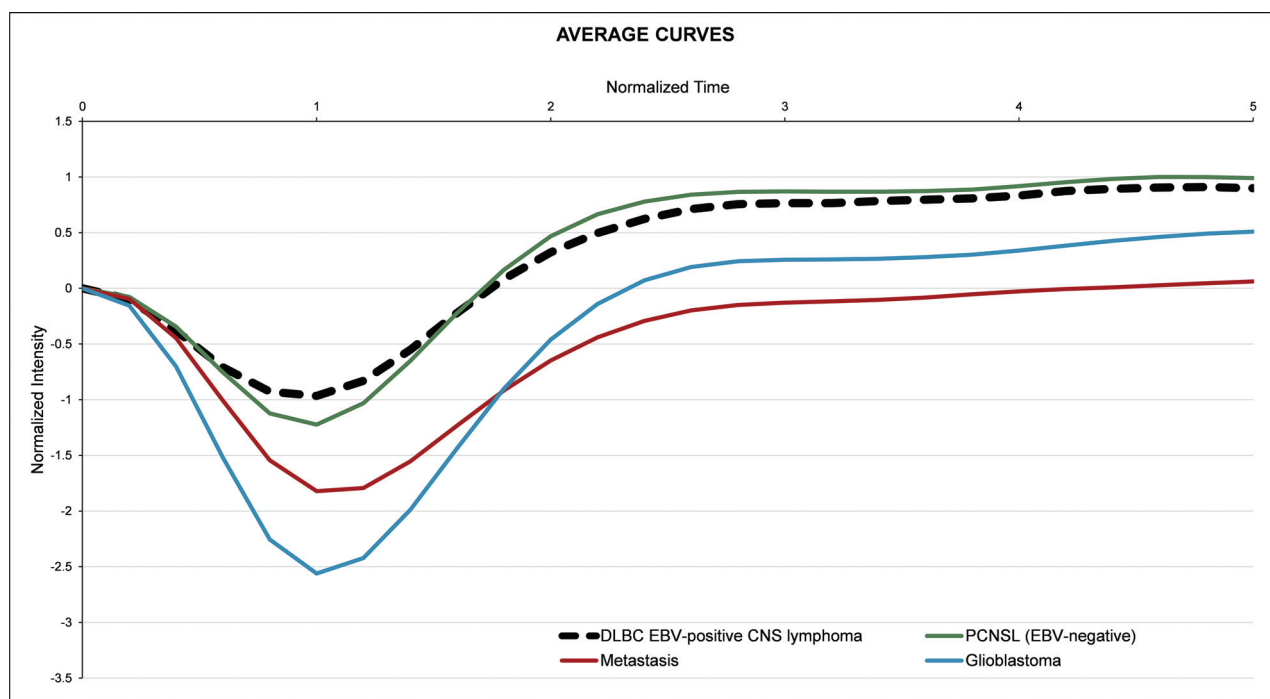


FIG 2. Average nTIC of DLBC EBV-positive CNS lymphoma, PCNSL (EBV-negative), metastasis, and glioblastoma. Few differences may be seen between DLBC EBV-positive CNS lymphoma and PCNSL. The most relevant visual differences between DLBC EBV-positive CNS lymphoma and metastasis or glioblastoma are seen around the maximal-signal-intensity drop and the signal-recovery segments of the curves.

Table 3: Summary of results

| | <i>P</i> ^a | AUC |
|-----------------|-----------------------|-------|
| nTIC algorithms | | |
| vs glioblastoma | <.001 | 0.984 |
| vs metastasis | <.001 | 0.898 |
| PSR | | |
| vs glioblastoma | .006 | 0.833 |
| vs metastasis | .002 | 0.873 |
| rCBV | | |
| vs glioblastoma | .003 | 0.855 |
| vs metastasis | .122 | 0.687 |

^a Statistical significance, Mann-Whitney *U* test.

analyze DLBC EBV-positive CNS lymphoma nTIC features and PSR values, to the best of our knowledge.

Currently, it is recognized that DLBC EBV-positive CNS lymphoma is a specific subtype of CNS lymphoma associated with immunodeficiency.^{8,15,16} AIDS-related CNS lymphoma appeared to become one of the most frequent brain tumors in the 1990s due to the explosion of the AIDS pandemic.³³ However, with the advent of antiretroviral therapies, AIDS-related CNS lymphoma has gradually decreased in the 2000s.^{34,35} Inherent to medical advances, other non-AIDS immunodeficiencies such as iatrogenic (posttransplantation and others), immunosenescence, and chronic inflammation have increased and probably overtaken AIDS as a cause of immunodeficiency-related CNS lymphoma.^{17-21,36} Also, due to the differing underlying physiopathologies of these conditions, strict monitoring of patients, and the improvement in imaging techniques, necrotic tumors have become the main radiologic differentials.^{14,37-39}

In the authors' opinion, radiology literature regarding DLBC EBV-positive CNS lymphoma without AIDS is scarce, probably due to the constantly evolving epidemiologic scenario and the relative rarity of the disease, making it difficult to pool these patients accurately.^{14,16-21,33-35,37-39} However, DLBC EBV-positive CNS lymphoma without AIDS is a clear and specific clinical immunobiologic entity that is challenging to diagnose because of the uncommon signatures for the much more frequent PCNSL and its great similarity to glioblastoma and metastasis on conventional imaging.^{14,37-39} Last, its identification before any surgical approach is crucial for optimal management because prompt biopsy without corticosteroids is the best choice, while surgical resection is not recommended.¹

In reference to the role of DSC-PWI, our literature search identified only 1 article that specifically assessed DSC-PWI of patients with DLBC EBV-positive CNS lymphoma without AIDS.¹⁰ Another article¹⁴ analyzed a subgroup of CNS lymphomas under the term "atypical PCNSL" in patients without AIDS. Lee et al¹⁰ specifically assessed rCBV values of patients with DLBC EBV-positive CNS lymphoma and compared them with those in patients who were EBV-negative. They did not find differences between EBV-positive and EBV-negative CNS lymphomas, while we found a slightly significant difference. On the other hand, Suh et al¹⁴ reported relevant differences in rCBV values between their patients with atypical PCNSL and glioblastoma, congruent with our results. Nevertheless, in both articles the DSC-PWI analysis remained limited to rCBV, and the absence of AIDS is considered enough to rule out immunodeficiency, which raises the question of whether CNS lymphomas included in these articles could actually be "other

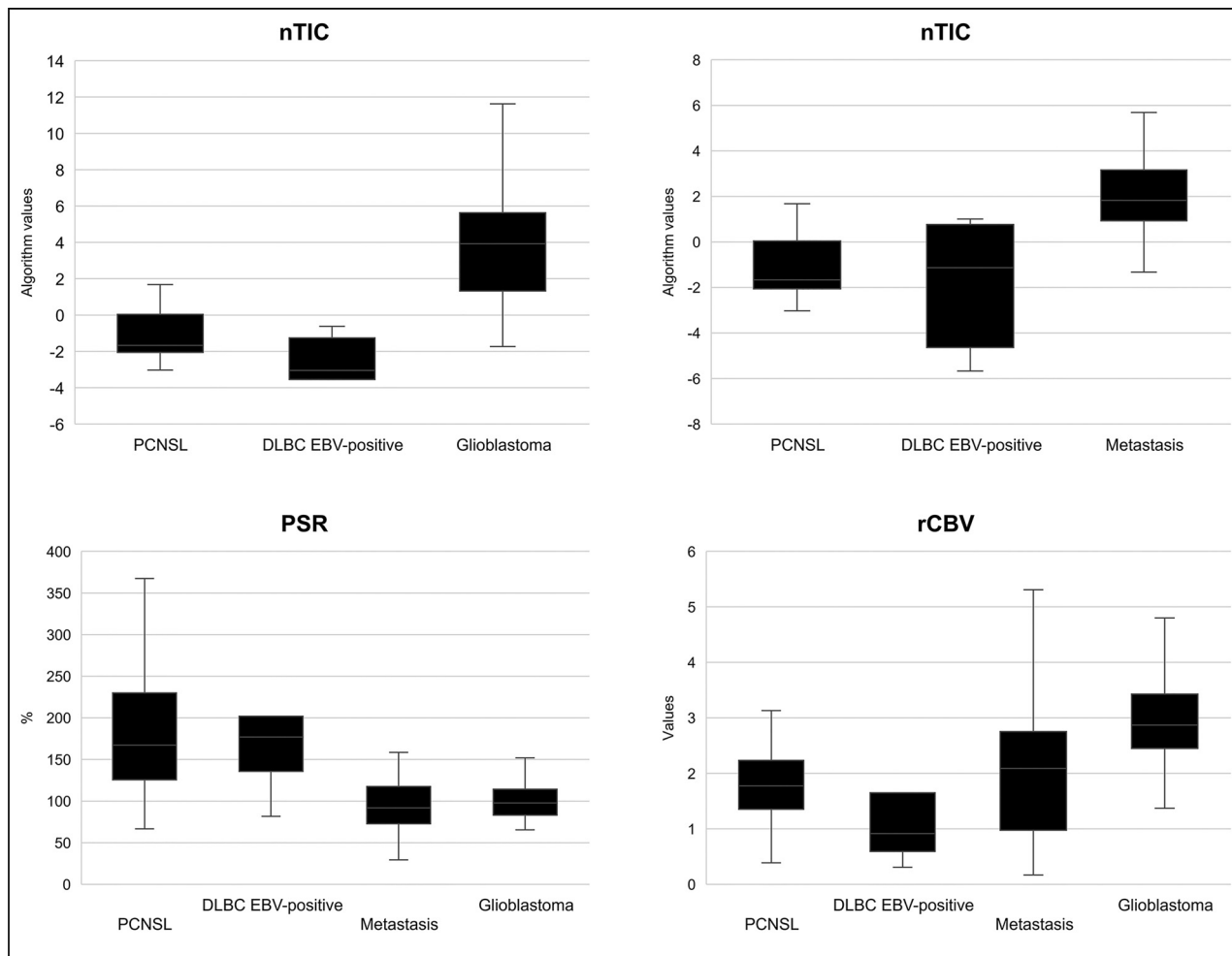


FIG 3. Boxplots depicting the results of the nTIC algorithms to differentiate PCNSL versus glioblastoma (*upper left*) and PCNSL versus metastasis (*upper right*) for each tumor subtype. *Lower row:* Boxplots depicting PSR and rCBV values for each tumor subtype.

immunodeficiency-associated,” such as ours. Finally, the mere comparison of EBV-positive and EBV-negative CNS lymphoma¹⁰ and the noninclusion of metastasis in the differential¹⁴ may condition the lack of clinically relevant information from our point of view and experience. To overcome these issues, we present a unique cohort with comprehensive clinical and demographic information and pathologic diagnosis according to the 2016 WHO lymphoid neoplasm¹⁵ and the 2021 WHO CNS tumor⁸ classifications, and we systematically describe conventional imaging and analyze the full potential of DSC-PWI to presurgically identify DLBC EBV-positive CNS lymphoma.

In this study, standard DSC-PWI metrics of PSR and rCBV achieved good or acceptable results in pair-wise discrimination of DLBC EBV-positive CNS lymphoma and glioblastoma or metastasis. Nonetheless, the application of previously reported nTICs analysis methodology²² yielded improved diagnostic performance. We mainly applied the previously published PCNSL presurgical classifier algorithms²² to our data set; but as a secondary analysis, we generated a dedicated algorithm to differentiate PCNSL and glioblastoma/metastasis as a whole group, also obtaining excellent results. Additionally, the curve-normalization process allows overlaying the averaged nTICs of relevant differential diagnoses

(Fig 2), which offers radiologist-friendly visual evaluation of curve differences. An additional advantage of the nTIC classifier results is the high-sensitivity levels provided, which is ideal in this scenario in which the most relevant goal is to raise suspicion of CNS lymphoma to avoid prebiopsy corticosteroids and potentially harmful tumor resection.²

DSC-PWI pulse-sequence parameters are known to influence CBV and PSR values, often paradoxically (ie, those sequences optimized for CBV calculations may be suboptimal for PSR and vice versa).⁴⁰ In this respect, we believe that the use of nTICs could be an alternative, especially in heterogeneous samples with nonstandardized technical acquisitions, which could be the situation among many neuroradiology departments worldwide such as ours because in this scenario, the evaluation of the whole normalized curve could surpass standard approaches such as CBV and PSR calculations.^{22,23}

On the other hand, in our experience, conventional imaging findings were insufficient to raise suspicion of CNS lymphoma because these tumors appear almost consistently as ring-enhancing necrotic lesions, with differing amounts of hemorrhage, mimicking glioblastoma or metastasis.⁹⁻¹⁴ We noted a prevalent heterogeneous low TSE-T2 signal from the central nonenhancing content of lesions,

not attributable to hemorrhage or calcification and, to the best of our knowledge, not usually seen in glioblastoma or metastasis.

Several considerations should be taken into account concerning this study. The single-site and retrospective character of the study may affect reproducibility. Nevertheless, they may also have conferred useful homogeneity to the study. Also, the limited number of cases of DLBC EBV-positive CNS lymphoma included may raise objections. However, this is a rare condition that needs to be detected presurgically, and the DSC-PWI characteristics have hardly been evaluated in the literature. At any rate, the data set suffices for a proof-of-concept demonstration, and our results warrant further multicentric prospective studies for validation. Furthermore, heterogeneous DSC-PWI technique acquisition parameters may compromise the generalizability of our concrete results. However, nTIC methodology is applicable elsewhere, and thresholds could be adapted in technically different cohorts.

Moreover, in our data set, no significant differences were found in nTICs among different DSC-PWI techniques, and indeed the nTIC method was created itself to hypothetically attenuate the impact of technical and physiologic variability on isolated parameter evaluation. Some of the data used in this investigation were part of previously published studies,^{22,23} but the aims of the study were clearly differentiated, and prior data were used for comparisons and differential diagnoses. Moreover, the use of previously published algorithms conferred a certain robustness on the study. Additionally, the reliability of data is ensured because they are available, well-balanced, curated, and filtered for prior publication. Finally, the absence of infection and brain abscess in the differential is a limitation. However, in our clinical experience with this data set of patients, glioblastoma and metastasis were the main differential diagnoses considered.

CONCLUSIONS

DSC-PWI could be very useful to presurgically differentiate DLBC EBV-positive CNS lymphoma and glioblastoma or metastasis. Among DSC-PWI metrics, nTIC curvology assessment could surpass the performance of standard PSR and rCBV measures. Neuroradiologists should be aware of any risk factors for immunodeficiency when facing a necrotic tumor in the brain. In the event of potential immunodeficiency, careful assessment of DSC-PWI may raise the suspicion of DLBC EBV-positive CNS lymphoma, which would drastically alter patient management.

ACKNOWLEDGMENTS

We thank CERCA Programme/Generalitat de Catalunya for institutional support.

Disclosure forms provided by the authors are available with the full text and PDF of this article at www.ajnr.org.

REFERENCES

- Chiavazza C, Pellerino A, Ferrio F, et al. **Primary CNS lymphomas: challenges in diagnosis and monitoring.** *Biomed Res Int* 2018;2018:3606970 [CrossRef Medline](#)
- Qian L, Tomuleasa C, Florian I-A, et al. **Advances in the treatment of newly diagnosed primary central nervous system lymphomas.** *Blood Res* 2017;52:159–66 [CrossRef Medline](#)
- Bühning U, Herrlinger U, Krings T, et al. **MRI features of primary central nervous system lymphomas at presentation.** *Neurology* 2001;57:393–96 [CrossRef Medline](#)
- Malikova H, Koubska E, Weichet J, et al. **Can morphological MRI differentiate between primary central nervous system lymphoma and glioblastoma?** *Cancer Imaging* 2016;16:40 [CrossRef Medline](#)
- Mansour A, Qandeel M, Abdel-Razeq H, et al. **MR imaging features of intracranial primary CNS lymphoma in immune competent patients.** *Cancer Imaging* 2014;14:22 [CrossRef Medline](#)
- Haldorsen IS, Espeland A, Larsson EM. **Central nervous system lymphoma: characteristic findings on traditional and advanced imaging.** *AJNR Am J Neuroradiol* 2011;32:984–92 [CrossRef Medline](#)
- Tang YZ, Booth TC, Bhogal P, et al. **Imaging of primary central nervous system lymphoma.** *Clin Radiol* 2011;66:768–77 [CrossRef Medline](#)
- WHO Classification of Tumours Editorial Board. *World Health Organization Classification of Tumours of the Central Nervous System*. 5th ed. International Agency for Research on Cancer; 2021
- Sauter A, Faul C, Bitzer M, et al. **Imaging findings in immunosuppressed patients with Epstein Barr virus-related B cell malignant lymphoma.** *AJR Am J Roentgenol* 2010;194:141–49 [CrossRef Medline](#)
- Lee HY, Kim HS, Park JW, et al. **Atypical imaging features of Epstein-Barr virus-positive primary central nervous system lymphomas in patients without AIDS.** *AJNR Am J Neuroradiol* 2013;34:1562–67 [CrossRef Medline](#)
- Jiménez de la Peña M del M, Vicente LG, Alonso RC, et al. **The multiple faces of nervous system lymphoma. Atypical magnetic resonance imaging features and contribution of the advanced imaging.** *Curr Probl Diagn Radiol* 2017;46:136–45 [CrossRef Medline](#)
- Lin X, Khan IRA, Seet YH, et al. **Atypical radiological findings of primary central nervous system lymphoma.** *Neuroradiology* 2020;62:669–76 [CrossRef Medline](#)
- Shin DJ, Lee EJ, Lee JE, et al. **Common and uncommon features of central nervous system lymphoma on traditional and advanced imaging modalities.** *Neurographics* 2017;7:437–49 [CrossRef](#)
- Suh CH, Kim HS, Lee SS, et al. **Atypical imaging features of primary central nervous system lymphoma that mimics glioblastoma: utility of intravoxel incoherent motion MR imaging.** *Radiology* 2014;272:504–13 [CrossRef Medline](#)
- Swerdlow SH, Campo E, Pileri SA, et al. **The 2016 revision of the World Health Organization classification of lymphoid neoplasms.** *Blood* 2016;127:2375–90 [CrossRef Medline](#)
- Gandhi MK, Hoang T, Law SC, et al. **EBV-associated primary CNS lymphoma occurring after immunosuppression is a distinct immunobiological entity.** *Blood* 2021;137:1468–77 [CrossRef Medline](#)
- Mahale P, Shiels MS, Lynch CF, et al. **Incidence and outcomes of primary central nervous system lymphoma in solid organ transplant recipients.** *Am J Transplant* 2018;18:453–61 [CrossRef Medline](#)
- Verdu-Bou M, Tapia G, Hernandez-Rodriguez A, et al. **Clinical and therapeutic implications of Epstein-Barr virus in HIV-related lymphomas.** *Cancers (Basel)* 2021;13:5534 [CrossRef Medline](#)
- Kaulen LD, Karschnia P, Dietrich J, et al. **Autoimmune disease-related primary CNS lymphoma: systematic review and meta-analysis.** *J Neurooncol* 2020;149:153–59 [CrossRef Medline](#)
- Mancuso S, Carlisi M, Santoro M, et al. **Immunosenescence and lymphomagenesis.** *Immun Ageing* 2018;15:22 [CrossRef Medline](#)
- Barosi G. **An immune dysregulation in MPN.** *Curr Hematol Malig Rep* 2014;9:331–39 [CrossRef Medline](#)
- Pons-Escoda A, Garcia-Ruiz A, Naval-Baudin P, et al. **Presurgical identification of primary central nervous system lymphoma with normalized time-intensity curve: a pilot study of a new method to analyze DSC-PWI.** *AJNR Am J Neuroradiol* 2020;41:1816–24 [CrossRef Medline](#)
- Pons-Escoda A, Garcia-Ruiz A, Naval-Baudin P, et al. **Voxel-level analysis of normalized DSC-PWI time-intensity curves: a potential generalizable approach and its proof of concept in discriminating glioblastoma and metastasis.** *Eur Radiol* 2022;32:3705–15 [CrossRef Medline](#)

24. Lee MD, Baird GL, Bell LC, et al. Utility of percentage signal recovery and baseline signal in DSC-MRI optimized for relative CBV measurement for differentiating glioblastoma, lymphoma, metastasis, and meningioma. *AJNR Am J Neuroradiol* 2019;40:1445–50 [CrossRef Medline](#)
25. Xing Z, You RX, Li J, et al. Differentiation of primary central nervous system lymphomas from high-grade gliomas by rCBV and percentage of signal intensity recovery derived from dynamic susceptibility-weighted contrast-enhanced perfusion MR imaging. *Clin Neuroradiol* 2014;24:329–36 [CrossRef Medline](#)
26. Neska-Matuszewska M, Bładowska J, Saósiadek M, et al. Differentiation of glioblastoma multiforme, metastases and primary central nervous system lymphomas using multiparametric perfusion and diffusion MR imaging of a tumor core and a peritumoral zone: searching for a practical approach. *PLoS One* 2018;13:e0191341 [CrossRef Medline](#)
27. Wang S, Kim S, Chawla S, et al. Differentiation between glioblastomas, solitary brain metastases, and primary cerebral lymphomas using diffusion tensor and dynamic susceptibility contrast-enhanced MR imaging. *AJNR Am J Neuroradiol* 2011;32:507–14 [CrossRef Medline](#)
28. Lee IH, Kim ST, Kim HJ, et al. Analysis of perfusion weighted image of CNS lymphoma. *Eur J Radiol* 2010;76:48–51 [CrossRef Medline](#)
29. Calli C, Kitis O, Yuntun N, et al. Perfusion and diffusion MR imaging in enhancing malignant cerebral tumors. *Eur J Radiol* 2006;58:394–403 [CrossRef Medline](#)
30. Mangla R, Kolar B, Zhu T, et al. Percentage signal recovery derived from MR dynamic susceptibility contrast imaging is useful to differentiate common enhancing malignant lesions of the brain. *AJNR Am J Neuroradiol* 2011;32:1004–10 [CrossRef Medline](#)
31. Boxerman JL, Schmainda KM, Weisskoff RM. Relative cerebral blood volume maps corrected for contrast agent extravasation significantly correlate with glioma tumor grade, whereas uncorrected maps do not. *AJNR Am J Neuroradiol* 2006;27:859–67 [Medline](#)
32. Cha S, Lupo JM, Chen MH, et al. Differentiation of glioblastoma multiforme and single brain metastasis by peak height and percentage of signal intensity recovery derived from dynamic susceptibility-weighted contrast-enhanced perfusion MR imaging. *AJNR Am J Neuroradiol* 2007;28:1078–84 [CrossRef Medline](#)
33. Corn BW, Marcus SM, Topham A, et al. Will primary central nervous system lymphoma be the most frequent brain tumor diagnosed in the year 2000? *Cancer* 1997;79:2409–13 [Medline](#)
34. Kadan-Lottick NS, Skluzacek MC, Gurney JG. Decreasing incidence rates of primary central nervous system lymphoma. *Cancer* 2002;95:193–202 [CrossRef Medline](#)
35. De Robles P, Fiest KM, Frolkis AD, et al. The worldwide incidence and prevalence of primary brain tumors: a systematic review and meta-analysis. *Neuro Oncol* 2015;17:776–83 [CrossRef Medline](#)
36. Adachi K, Yamaguchi F, Node Y, et al. Neuroimaging of primary central nervous system lymphoma in immunocompetent patients: comparison of recent and previous findings. *J Nippon Med Sch* 2013;80:174–83 [CrossRef Medline](#)
37. Wang ZD, Liu HH, Ma ZX, et al. Toxoplasma gondii infection in immunocompromised patients: a systematic review and meta-analysis. *Front Microbiol* 2017;8:1–12 [CrossRef Medline](#)
38. Arendt G, Maschke M. Update: opportunistic infections of the central nervous system in patients with iatrogenic immunosuppression: an update. *Neurology International Open* 2017;1:E316–25 [CrossRef](#)
39. Morollón N, Rodríguez F, Duarte J, et al. Brain lesions in a long-term kidney transplant recipient: primary cerebral lymphoma or cerebral toxoplasmosis? *Neurologia* 2017;32:268–70 [CrossRef Medline](#)
40. Cindil E, Sendur HN, Cerit MN, et al. Validation of combined use of DWI and percentage signal recovery-optimized protocol of DSC-MRI in differentiation of high-grade glioma, metastasis, and lymphoma. *Neuroradiology* 2021;63:331–42 [CrossRef Medline](#)